ELSEVIER

Journal of Hazardous Materials B125 (2005) 205–210

Journal of Hazardous Materials

www.elsevier.com/locate/jhazmat

Application of artificial neural networks for modeling of the treatment of wastewater contaminated with methyl *tert*-butyl ether (MTBE) by UV/H_2O_2 process

D. Salari [a,*], N. Daneshvar [b,1], F. Aghazadeh [a,2], A.R. Khataee [b,3]

[a] *Petroleum Research Laboratory, Department of Applied Chemistry, Faculty of Chemistry, University of Tabriz, Tabriz, Iran*

[b] *Water and Wastewater Treatment Research Laboratory, Department of Applied Chemistry, Faculty of Chemistry, University of Tabriz, Tabriz, Iran*

Received 9 March 2005; received in revised form 18 May 2005; accepted 24 May 2005
Available online 5 July 2005

Abstract

During the last two decades, methyl *tert*-butyl ether (MTBE) has been widely used as an additive to gasoline (up to 15%) both to increase the octane number and as a fuel oxygenate to improve air quality by reducing the level of carbon monoxide in vehicle exhausts. The present work mainly deals with photooxidative degradation of MTBE in the presence of H_2O_2 under UV light illumination (30 W). We studied the influence of the basic operational parameters such as initial concentration of H_2O_2 and irradiation time on the photodegradation of MTBE. The oxidation rate of MTBE was low when the photolysis was carried out in the absence of H_2O_2 and it was negligible in the absence of UV light. The addition of proper amount of hydrogen peroxide improved the degradation, while the excess hydrogen peroxide could quench the formation of hydroxyl radicals ($^{\bullet}$OH). The semi-log plot of MTBE concentration versus time was linear, suggesting a first order reaction. Therefore, the treatment efficiency was evaluated by figure-of-merit electrical energy per order (E_{Eo}). Our results showed that MTBE could be treated easily and effectively with the UV/H_2O_2 process with E_{Eo} value 80 kWh/m^3/order. The proposed model based on artificial neural network (ANN) could predict the MTBE concentration during irradiation time in optimized conditions. A comparison between the predicted results of the designed ANN model and experimental data was also conducted.

Keywords: Advanced oxidation processes; Artificial neural networks; MTBE; Fuel oxygenate; Electricity consumption

1. Introduction

Methyl *tert*-butyl ether (MTBE) is a fuel additive made, in part, from natural gas. Since 1979, it has been used as an octane enhancing replacement for tetraethyl lead in gasoline [1]. Increased oxygen content is required to improve combustion efficiency and reduce harmful tailpipe emissions, such as CO, O_3, etc., from motor vehicles. To achieve the specified oxygen content requirements, 5–15% MTBE in gasoline is required [2].

Since MTBE has high water solubility, the occurrence of fuel spills or leaks from underground storage tanks or transferring pipeline has led to the contamination of natural waters. The United States Environmental Protection Agency (EPA) has classified MTBE as a suspect human carcinogen and issued a draft lifetime health advisory limit of 20–30 ppb MTBE in drinking water [1,3].

* Corresponding author. Tel.: +98 411 3393149; fax: +98 411 3340191.
E-mail addresses: drshsalari@yahoo.com (D. Salari), nezam_daneshvar@yahoo.com (N. Daneshvar), Faezeh_chem@hotmail.com (F. Aghazadeh), a.khataee@tabrizu.ac.ir (A.R. Khataee).
[1] Tel.: 98 411 3393146; Fax: 98 411 3393038.
[2] Tel.: 98 411 3393149; Fax: 98 411 3340191.
[3] Tel.: 98 411 3393165; Fax: 98 411 3393038.

0304-3894/$ – see front matter © 2005 Elsevier B.V. All rights reserved.
doi:10.1016/j.jhazmat.2005.05.030

In general, the presence of MTBE complicates remediation attempts. Conventional treatment of MTBE-contaminated groundwater is inefficient and unsatisfactory. Air stripping is difficult and requires a high air-to-water ratio (>200/1 for 5% removal), because of its very low Henry's law constant. The low affinity of MTBE towards granular activated carbon makes this process undesirable and expensive [4]. It can be treated biologically with specific bacterial strains or natural isolates under aerobic condition. However, the bacteria grow slowly with low yields of bio-mass and are sometimes unstable. As a result, a viable bio-remediation process for MTBE has not been completely developed [5,6]. Therefore, it is necessary to introduce an effective method in order to complete removal of MTBE from contaminated waters. In recent years, an alternative to conventional methods, is "advanced oxidation processes" (AOPs), based on the generation of very reactive species such as hydroxyl radicals that oxidize a broad range of organic pollutants quickly and nonselectively [7–9].

There are several AOPs studies for MTBE treatment, such as UV/H_2O_2 [10–12], O_3/H_2O_2 [5,13], photo-Fenton process [14,15] and UV/TiO_2 [3,4]. The intermediate by-products were identified and the oxidation mechanism was also elucidated [1,12,15].

Due to the complexity of the reactions of UV/H_2O_2 system, a few studies have been conducted involving the kinetics of the destruction of MTBE by UV/H_2O_2 process. To our knowledge, Safarzadeh-Amiri and co-workers [11] proposed the kinetic model based on the initial rates of destruction of MTBE. Chang and Young [12] investigated the kinetics of UV/peroxide process in a way that can be generalized for design purposes. Artificial neural networks (ANN) are a promising alternative modeling technique. The phenomenological treatment of a photochemical system is, in general, quite complex. This is caused by the complexity of solving the equations that involve the radiant energy balance, the spatial distribution of the absorbed radiation, mass transfer, and the mechanisms of a photochemical degradation involving radical species. Due to these reasons, the modeling of the degradation process via artificial neural network techniques is quite appropriate [16–19]. One of the characteristics of modeling based on artificial neural networks is that it does not require the mathematical description of the phenomena involved in the process, and might therefore prove useful in simulating and up-scaling complex photochemical systems. The success in obtaining a reliable and robust network depends strongly on the choice of process variables involved as well as the available set of data and the domain used for training purposes [20]. Therefore, the aim of the experiments was to investigate the influence of various parameters on photooxidative degradation of MTBE to optimize the effective parameters. An important objective was to obtain an ANN model that could make reliable prediction of the efficiency of the destruction process.

2. Experimental

2.1. Materials

MTBE was obtained from Merck (99%). Hydrogen peroxide (30%, w/w), hydrochloric acid and sodium hydroxide were purchased from Aldrich and used without further purification.

2.2. General procedure

For the UV/H_2O_2 process, irradiation was carried out with a 30 W (UV-C) mercury lamp (Philips), which was put above a batch photoreactor of 500 ml in volume. The distance between solution and UV source was constant, 15 cm, in all experiments. The desired concentration of MTBE and H_2O_2 were fed into the Pyrex reactor. The solution pH values were adjusted at desired level using dilute NaOH and HCl and then the pH values were measured with pH meter (Philips PW 9422). After that, the lamp was switched on to initiate the reaction. During irradiation, the aqueous solution was magnetically stirred and the solution was sampled after an appropriate illumination time. The concentration of MTBE in each degraded sample was determined with a gas chromatograph.

2.3. Analytical method

MTBE was analyzed by a CP-9001 (CROMPAK) gas chromatograph (GC) equipped with a flame ionization detector (FID). A CP Wax (CP-WAX 58CB) column (50 m × 0.32 mm, 1.2 μm film thickness) in connection with the FID detector was used. The temperature was programmed at 50 °C for 10 min, then to 120 °C at a rate of 5 °C/min, and held at 120 °C for 5 min; N_2 was the carrier gas. The injector port temperature was 180 °C, and the samples were injected in the split injection mode.

2.4. ANN software

All ANN calculations carried out using Matlab 6.5 mathematical software with ANN toolbox for windows running on a personal computer (Pentium IV 2800 MHz). A three-layer network with a sigmoidal transfer function (trainscg) with back propagation algorithm was designed in this study.

3. Results and discussion

3.1. Effect of UV irradiation in the presence of H_2O_2

Fig. 1 shows the concentration of MTBE against time for experiments carried out under UV irradiation only, hydrogen peroxide without UV irradiation and UV irradiation in the presence of hydrogen peroxide. It can be seen from the figure that in the presence of both H_2O_2 and UV light, 100% of

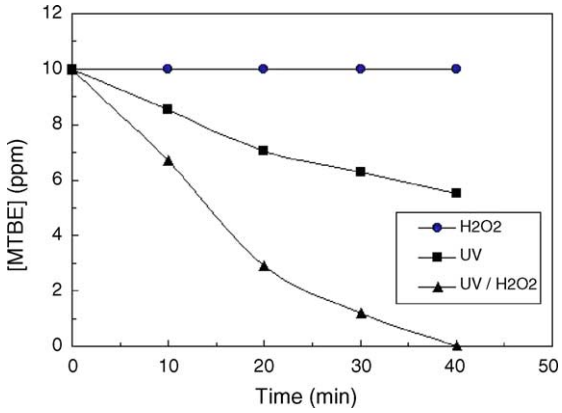

Fig. 1. Effect of UV light and H_2O_2 on photodegradation of MTBE. $[MTBE]_o = 10$ ppm, $[H_2O_2]_o = 60$ ppm, pH = 6.5.

MTBE was degraded at the irradiation time of 40 min. This was contrasted with 44% destruction for the same experiment performed in the absence of H_2O_2, and the negligible when the UV lamp had been switched off and the reaction was allowed to occur in the darkness. These experiments demonstrated that both UV light and an oxidizing agent, such as H_2O_2 were needed for the effective destruction of MTBE. The presumed reason is that degradation of MTBE is due to the hydroxyl radicals generated upon photolysis of hydrogen peroxide according to the following reactions [21,22]:

$$H_2O_2 + h\nu \rightarrow 2^{\bullet}OH \quad (1)$$

$$H_2O_2 + {}^{\bullet}OH \rightarrow HO_2^{\bullet} + H_2O \quad (2)$$

$$H_2O_2 + {}^{\bullet}O_2H \rightarrow {}^{\bullet}OH + H_2O + O_2 \quad (3)$$

$$HO_2^{\bullet} + {}^{\bullet}OH \rightarrow H_2O + O_2 \quad (4)$$

The hydroxyl radical is a powerful oxidizing agent and attacks MTBE molecule by abstracting a hydrogen atom from either the methoxy group or any of the three equivalent methyl groups to form carbon-centered radicals [10].

3.2. Effect of initial hydrogen peroxide concentration

Hydrogen peroxide concentration is an important parameter for the degradation of the pollutants in the UV/H_2O_2 process. The photodestruction of MTBE has been studied at different hydrogen peroxide concentrations. Our results showed that this reaction followed a pseudo-first-order kinetics and that the reaction rate constant was a function of the peroxide concentration. Results are given in Figs. 2 and 3.

According to the Fig. 3, as H_2O_2 concentration increases the destruction of MTBE is accelerated up to 60 mg/l, but above it, the destruction rate decreases. This is due to the fact that more hydroxyl radicals are formed as H_2O_2 concentration increases (Eq. (1)). However, it should be noticed that as the H_2O_2 concentration is over 60 mg/l, for example, 100 mg/l, no further acceleration in the destruction of MTBE was observed. This is due to the fact that at a higher H_2O_2

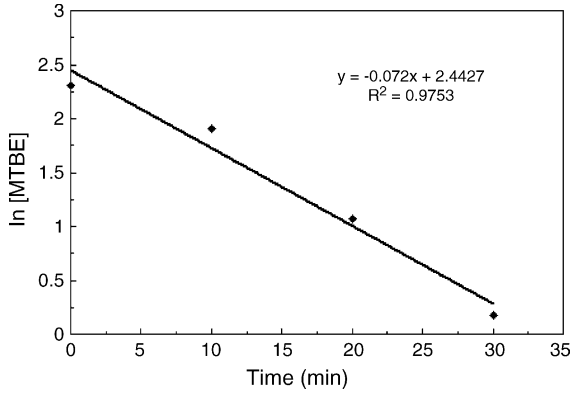

Fig. 2. Relationship between ln [MTBE] and irradiation time on photodegradation of MTBE. $[MTBE]_o = 10$ ppm, $[H_2O_2]_o = 60$ ppm, pH = 6.5.

concentration, scavenging of hydroxyl radicals will occur, which can be expressed by the Eqs. (2) and (4) [7,22].

Since $HO_2^{\bullet}$ is less reactive than ${}^{\bullet}OH$, increased amount of hydrogen peroxide has a diminishing return on the reaction rate. Therefore, it is important to optimize the applied dose of hydrogen peroxide to maximize the performance of the UV/H_2O_2 process and minimize the treatment cost [8].

3.3. Electrical energy determination

Since photodegradation of aqueous organic pollutant is an electric-energy-intensive process, and electric energy can represent a major fraction of the operating costs, simple figures-of-merit based on electric energy consumption can be very useful and informative. Recently, the Photochemistry Commission of the International Union of Pure and Applied Chemistry (IUPAC) proposed a figure-of-merit (or more appropriately, an efficiency index, as it compares electrical efficiency of different AOPs) for UV-based AOPs [22]. It compares electrical efficiency of different UV-based AOPs and is a measure of the electrical efficiency of an AOP system. It is defined (for low concentration of pollutants) as the electrical energy in kilowatt hours (kWh) required bringing about the degradation of a contaminant by one order of magnitude in 1 m^3 (1000 l) of contaminated water [23].

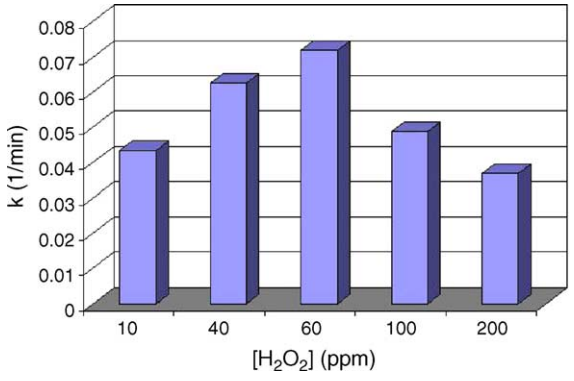

Fig. 3. Effect of initial concentration of H_2O_2 on photodegradation of MTBE. $[MTBE]_o = 10$ ppm, pH = 6.5.

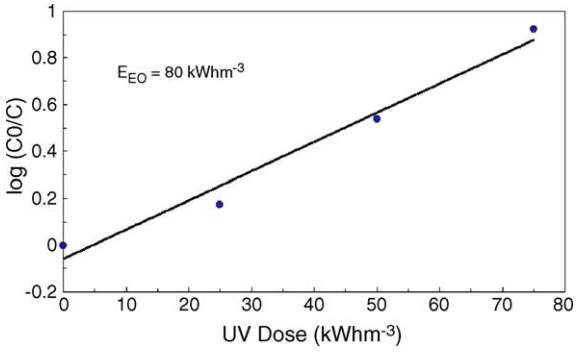

Fig. 4. E_{Eo} determination for photodegradation of MTBE by UV/H_2O_2 process. $[MTBE]_o$ = 10 ppm, $[H_2O_2]_o$ = 60 ppm.

Considering first-order destruction kinetics, the UV dose was calculated for UV/H_2O_2 process using Eq. (5) [9,24]. The electrical energy per order (E_{Eo}) values was obtained from the inverse of the slope of a plot of log (C_0/C) versus energy dose (kWh/m^3) (see Fig. 4).

$$\text{UV dose} = \frac{1000 \times \text{lamp power (kW)} \times \text{time (h)}}{\text{treated volume (l)}} \quad (5)$$

The electric dose (kWh/m^3) required to oxidize MTBE (10 ppm) in the presence of 60 ppm H_2O_2 at different reaction times was calculated from the kinetic data (Fig. 4). The calculated dose considers the electric power of the lamp (30 W) and the total volume of the reactor (200 ml) at the irradiation time of 40 min.

Finally, it is useful to relate the E_{Eo} values found in this study to treatment costs. For instance, if the treatment objective for MTBE ($[MTBE]_o$ = 10 mg/l) is 1.2 mg/l, this means a log reduction of 0.921 and hence, the total electrical energy required is 81.433 kWh/m^3. If the cost of electricity, in Iran, is US$ 0.0065 per kWh, the contribution to treatment cost from electrical energy will be US$ 0.5298 per m^3. In addition, there will be smaller cost factors for the hydrogen peroxide used and for lamp replacement.

3.4. Neural network modeling

ANNs are direct inspiration from the biology of human brain, where billions of neurons are interconnected to process a variety of complex information. Accordingly, a computational neural network consists of simple processing units called neurons. In general, a neural net, as shown in Fig. 5, is parallel interconnected structure consisting of: (1) input layer of neuron (independent variables), (2) a number of hidden layers and (3) output layer (dependent variables). The number of input and output neurons is determined by the nature of the problem. The hidden layers act like feature detectors and in theory, there can be more than one hidden layer. Universal approximation theory, however, suggests that a network with a single hidden layer with a sufficiently large number of neurons can interpret any input–output structure [18].

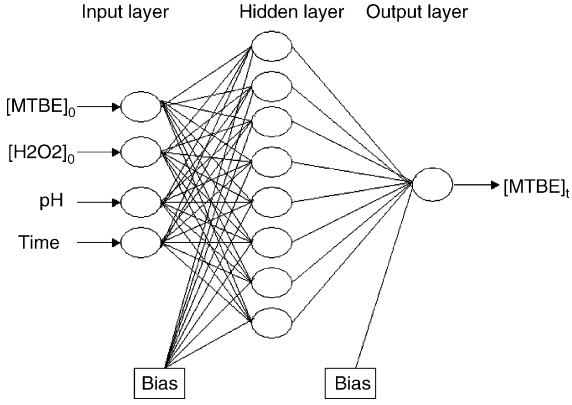

Fig. 5. The ANN optimized structure.

The topology of an artificial neural network (ANN) is determined by the number of layers in the ANN, the number of nodes in each layer and the nature of the transfer functions. Optimization of ANN topology is probably the most important step in the development of a model. We used three-layered feed forward back propagation neural network (4:8:1) for modeling of MTBE photodegradation (Fig. 5). In the present work, the input variables to the feed forward neural network were as follows: the reaction time (t), the initial concentration of MTBE, the initial concentration of H_2O_2 and pH of the solution. The concentration of MTBE, as a function of reaction time ([MTBE]t), was chosen as the experimental response or output variable.

In order to determine the optimum number of hidden nodes, a series of topologies was used, in which the number of nodes was varied from 2 to 10. Each topology was repeated three times to avoid random correlation due to the random initialization of the weights. Fig. 6 illustrates the relation between the network error and the number of neurons in the hidden layer. The mean square error (MSE) was used as the error function. MSE measures the performance of the

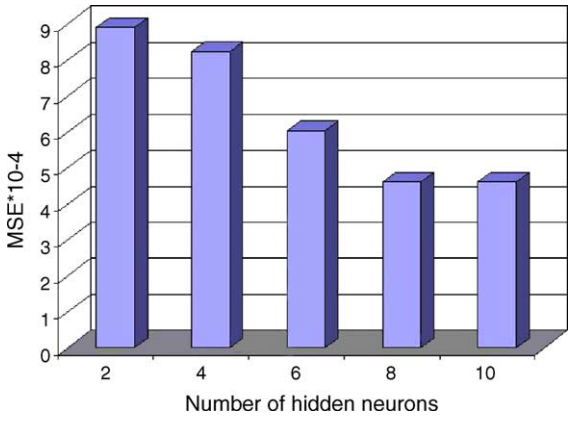

Fig. 6. Effect of the number of neurons in hidden layer on the performance of the neural network.

Table 1
Model variables and their ranges

Variable	Range
Input layer	
Reaction time (min)	0–60
pH	2.5–12
Initial concentration of MTBE (ppm)	0–36
Initial concentration of H_2O_2 (ppm)	0–100
Output layer	
Concentration of MTBE (ppm)	0–36

network according to the following equation:

$$\mathrm{MSE} = \frac{1}{Q\sum_{i=1}^{Q}(y_{\mathrm{nn}} - y_{\mathrm{expl}})^2} \quad (6)$$

where Q is the number of data point, y_{nn} the network prediction, y_{expl} experimental response and i is an index of data. We can see that the performance of the network stabilized after inclusion of an adequate number of hidden units just about eight. The network with too few neurons in the hidden layer cannot converge effectively.

In this work, the sigmoidal transfer function was used as a transfer function in the hidden and output layers. This is the most widely used transfer function, which is given by:

$$f(x) = \frac{1}{1 + \exp(-x)} \quad (7)$$

where $f(x)$ is the hidden neuron output [18]. The training function was *trainscg*. Out of the several data points generated, 64 experimental sets were used to feed the ANN structure. The range of variables studied is summarized in Table 1. The samples were splitted into training, validation and test subsets that each of them contains 32, 16 and 16 samples, respectively. The validation and test sets, for evaluation of the validation and modeling power of the model, were randomly selected from the experimental data. Since the used transfer function in the hidden layer was sigmoid, all samples must be scaled into the 0.2–0.8. So any samples (X_i) (from the training, validation and test sets) were scaled to a new value A_i as follows:

$$A_i = 0.2 + \frac{0.6(X_i - \min(X_i))}{\max(X_i) - \min(X_i)} \quad (8)$$

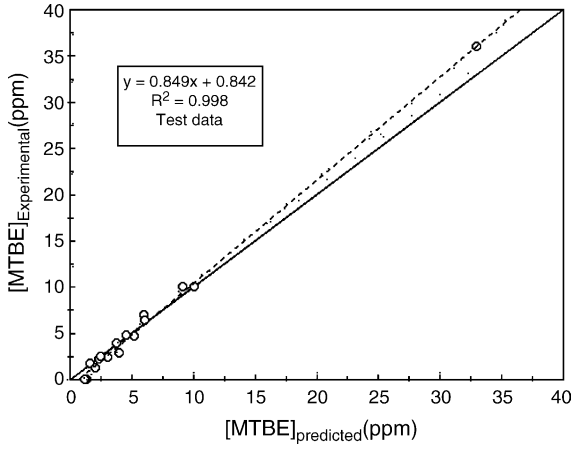

Fig. 7. Comparison of the experimental results with those calculated via neural network modeling for the test sets.

where $\min(X_i)$ and $\max(X_i)$ are the extreme values of variable X_i [20].

Of course, to calculate training, validation and test errors, all of the outputs were performed an inverse range scaling to return the predicted responses to their original scale and compared them with experimental responses. A neural network with eight neurons in the hidden layer was used with 800 iterations, providing the weights listed in Table 2.

Fig. 7 shows a comparison between calculated and experimental values of the output variable ([MTBE]t) for test sets, using the neural network model with number of hidden layer equal to eight. We used two lines to show the success of the prediction. The one is the perfect fit (predicted data equal to experimental data), on which all the data of an ideal model should lay. The other line is the line that best fits on the data of the scatter plot with equation $Y = ax + b$ and it is obtained with regression analysis based on the minimization of the squared errors. The correlation coefficient of this line is also presented (R^2). The closer to 1 this factor is and the closer the coefficients of the line to 1 and 0, respectively, are the better the model is. The plot in this figure has correlation coefficient of 0.998 for the test set. These results confirm that the neural network model reproduces the photodegradation of MTBE

Table 2
Matrices of weights, W1: weights between input and hidden layers; W2: weights between hidden and output layers

W1						W2	
Neuron	Variable				Bias	Neuron	Weight
	Time	$[\mathrm{MTBE}]_o$	pH	$[\mathrm{H_2O_2}]_o$			
1	5.3666	5.1934	4.7207	−12.7819	−7.1101	1	0.1517
2	0.0836	−0.7260	14.6596	1.8335	−13.133	2	−0.8678
3	6.8655	−8.9152	10.2480	4.2958	−9.5076	3	0.4948
4	1.5783	3.7490	−9.2868	11.4560	1.0073	4	−0.8060
5	−17.3715	−0.5233	−3.1753	6.5619	2.9307	5	0.5939
6	12.2281	−3.8027	1.2883	3.2496	−2.8009	6	−2.6415
7	16.5064	3.3394	−4.3147	0.6189	4.0552	7	−0.1373
8	12.3280	11.2680	2.4224	5.9807	−7.1996	8	1.7258
						Bias	0.4329

in our system, within the experimental ranges adopted in the model fitting.

4. Conclusion

The UV/H_2O_2 system has been demonstrated to be efficient process for the oxidation of MTBE in aqueous solution. Photooxidative degradation efficiency of MTBE was small when photolysis was carried out in the absence of H_2O_2. The results indicated that the degree of photodegradation of MTBE was obviously affected by the initial concentration of H_2O_2. We found that the optimal amount of H_2O_2 was 60 ppm, with MTBE concentration of 10 ppm. The electrical energy per order (E_{Eo}) and cost of the required electrical energy was calculated. Artificial neural network modeling has been used to investigate the cause effect relationship prevalent in photooxidation process of MTBE. The ANN model could describe the behavior of the complex reaction system (UV/H_2O_2 process) with the range of experimental conditions adopted. Simulation based on the ANN model can then be performed in order to estimate the behavior of the system under different conditions. This information is essential for the adequate scale-up and design of industrial scale batch reactors for the treatment of organic contaminants in wastewaters.

Acknowledgments

The authors thank the University of Tabriz, Iran, for financial and other supports.

References

[1] M. Stefan, J. Mack, J. Bolton, Degradation pathways during the treatment of methyl *tert*-butyl ether by the UV/H_2O_2 process, Environ. Sci. Technol. 34 (2000) 650–658.
[2] W. Dekant, U. Bernauer, E. Rosner, A. Amberg, Toxicokinetics of ethers used as fuel oxygenates, Toxicol. Lett. 124 (2001) 37–45.
[3] Y. Zang, R. Farnood, Photocatalytic decomposition of methyl *tert*-butyl ether in aqueous slurry of titanium dioxide, Appl. Catal. B 57 (2004) 273–279.
[4] R. Barreto, K. Gray, K. Anders, Photocatalytic degradation of methyl-*tert*-butyl ether in TiO_2 slurries: a proposed reaction scheme, Water Res. 29 (1995) 1243–1248.
[5] A. Safarzadeh-Amiri, O_3/H_2O_2 treatment of methyl-*tert*-butyl ether in contaminated waters: effect of background COD on the O_3-dose, Ozone Sci. Eng. 24 (2001) 55–62.
[6] C. Guillard, N. Charton, P. Pichat, Degradation mechanism of t-butyl methyl ether (MTBE) in atmospheric droplets, Chemosphere 53 (2003) 469–477.
[7] N. Daneshvar, D. Salari, A.R. Khataee, Photocatalytic degradation of azo dye acid red 14 in water: investigation of the effect of operational parameters, J. Photochem. Photobiol. A 157 (2003) 111–116.
[8] N. Daneshvar, D. Salari, A.R. Khataee, Photocatalytic degradation of azo dye acid red 14 in water on ZnO as an alternative catalyst to TiO_2, J. Photochem. Photobiol. A 162 (2004) 317–322.
[9] N. Daneshvar, A. Aleboyeh, A.R. Khataee, The evaluation of electrical energy per order (EEo) for photooxidative decolorization of four textile dye solutions by the kinetic model, Chemosphere 59 (2005) 761–767.
[10] Y. Zang, R. Farnood, Effects of hydrogen peroxide concentration and ultraviolet light intensity on methyl *tert*-butyl ether degradation kinetics, Chem. Eng. Sci. 60 (2005) 1641–1648.
[11] S.R. Cater, M.I. Stefan, J.R. Bolton, A. Safarzadeh-Amiri, UV/H_2O_2 treatment of methyl *tert*-butyl ether in contaminated waters, Environ. Sci. Technol. 34 (2000) 659–662.
[12] P.B.L. Chang, T.M. Young, Kinetics of methyl *tert*-butyl ether degradation and by-product formation during UV/hydrogen peroxide water treatment, Water Res. 34 (2000) 2233–2240.
[13] A. Safarzadeh-Amiri, O_3/H_2O_2 Treatment of methyl-*tert*-butyl ether (MTBE) in contaminated waters, Water Res. 35 (2001) 3706–3714.
[14] A. Safarzadeh-Amiri, J.R. Bolton, S.R. Cater, Ferrioxalate-mediated photodegradation of organic pollutants in contaminated water, Water Res. 31 (1997) 787–798.
[15] A. Safarzadeh-Amiri, J.R. Bolton, S.R. Cater, Ferrioxalate-mediated solar degradation of organic contaminants in water, Sol. Energy 56 (1996) 439–443.
[16] S. Gob, E. Oliveros, S.H. Bossmann, A.M. Braun, R. Guardani, C.A.O. Nascimento, Modeling the kinetics of a photochemical water treatment process by means of artifical neual networks, Chem. Eng. Process. 38 (1999) 373–382.
[17] J.E.F. Moraes, F.H. Quina, C.A.O. Nascimeto, D.N. Silva, O. Chiavone-Filho, Treatment of saline wastewater contaminated with hydrocarbons by the photo-fenton process, Environ. Sci. Technol. 38 (2004) 1183–1187.
[18] V.K. Pareek, M.P. Brungs, A.A. Adesina, R. Sharma, Artificial neural network modeling of a multiphase photodegradation system, J. Photochem. Photobiol. A 149 (2002) 139–146.
[19] J.A. Stegemann, N.R. Buenfeld, Prediction of leachate pH for cement paste containing pure metal compounds, J. Hazard. Mater. B 90 (2002) 169–188.
[20] F. Despange, D.L. Massart, Neural networks in multivariate calibration, Analyst 123 (1998) 157–178.
[21] N. Daneshvar, M. Rabbani, N. Modirshahla, M.A. Behnejady, Photooxidative degradation of acid red 27 in a tubular continuous-flow photoreactor: influence of operational parameters and mineralization products, J. Hazard. Mater. B 18 (2005) 155–160.
[22] N. Daneshvar, M.J. Hejazi, B. Rangarangy, A.R. Khataee, Photocatalytic degradation of an aqueous suspensions of titanium dioxide, J. Environ. Sci. Health B 39 (2004) 285–296.
[23] J.R. Bolton, K.G. Bircher, W. Tumas, C.A. Tolman, Figures-of-merit for the technical development and application of advanced oxidation technologies for both electric-and solar-driven systems, Pure Appl. Chem. 73 (2001) 627–637.
[24] C. Lizama, M.C. Yeber, J. Freer, J. Baeza, H.D. Mansilla, Reactive dyes decolouration by TiO_2 photo-assisted catalysis, Water Sci. Technol. 44 (2001) 197–203.